JOURNAL OF ENGINEERING SCIENCES

Volume 11, Issue 2 (2024)

Shaik H. S. (2024). Kinematic analysis of 3-PRPPS spatial parallel manipulator with circularly guided base for singularity-free robotic motions. Journal of Engineering Sciences (Ukraine), Vol. 11(2), pp. A30–A39. https://doi.org/10.21272/jes.2024.11(2).a4

Kinematic Analysis of 3-PRPPS Spatial Parallel Manipulator with Circularly Guided Base for Singularity-Free Robotic Motions

Shaik H. S.*[0000-0003-0059-0285]

Vignan's Foundation for Science, Technology and Research, Vadlamudi, Guntur-522213, Hyderabad, India

Article info:
Submitted: July 25, 2024
Received in revised form: September 4, 2024
Accepted for publication: September 18, 2024
Available online: September 25, 2024

***Corresponding email:**
drsh_mech@vignan.ac.in

Abstract. Robot manipulators are classified as serial manipulators and parallel manipulators. Parallel manipulators are classified into planar and spatial parallel manipulators (SPMs). The parallel manipulators have moved and fixed platforms connected with serial chains. The parallel manipulators have many linkages, which create a singularity problem. The singular positions of SPMs have also gained substantial attention in various industrial applications due to their intrinsic advantages in precision, flexibility, and load-bearing capabilities. The 3-PRPPS SPM has three prismatic joints, one spherical joint, and one revolute joint. This work changed the fixed base with a circular guided base to avoid singularity issues. The manipulator was modeled with direct kinematic relations. The Jacobian matrix for position and orientation was derived. The workspace was taken as the common area of the three circles, whose radius was the maximum arm length. The position and orientation of the end effector were traced. In the form of the end effector traces, no singularities in the mechanism were observed. The path of the robot manipulator was observed in all the possible positions and orientations. The multi-body simulation was also conducted on the 3-PRPPS manipulator, the main findings of which are presented in this article.

Keywords: process innovation, automation, workspace, kinematic analysis, multi-body simulation, Jacobian matrix, production quality.

1 Introduction

In recent trends of automation of production lines, robot manipulators have played a vital role in industrial automation. Robots' targeted purposes are to increase productivity and production quality compared to human-produced goods with non-avoidable human errors. The present configurations of the robot manipulators suffer from unavoidable conditions inside the workspace, i.e., the working region of the robot is called singularity.

These singularities have a finite number of possibilities based on the numerical and orientation data, which can be predetermined to avoid these configurations of the manipulators and the position of the end effectors where the voids occur. These particular conditions, referred to as singularities, suffer from factors such as low reachability, high torque ratio, prone to failure of the entire system, and involve changing the working behavior [1–3].

These points where the robot voids occur are avoided during the workspace defining stage, and the positions of the workpiece are changed based on these void regions.

Due to the presence of these voids in the manipulator's configuration, most robot applications are based on point-to-point actions, continuous paths that suffer from positions in between the trajectory, which affects the manipulator during actuation [4].

Even during the manipulator's point-to-point actions, these singular configurations are avoided. The nature of the robot's design, i.e., robot types, plays a significant role in occurrences of this singular position [5]. Among these two robot design, the parallel manipulators are most affected during actuation with the presence of singular regions. Major robotic researchers and scholars are working towards avoiding these singularities in their works.

This research was initiated to bring out the most possible and feasible mechanism that can be easily implemented in the existing manipulator. Adding a slight

change in the position of the base of the arm in a parallel manipulator changes the nature of singular region occurrence in the workspace through the introduction of redundant links in the manipulator.

The changes are significantly more significant when all the arms in the parallel manipulator are reoriented during actuation [6]. With these phenomena illustrated by scholars [7], the proposed 3-PRPPS spatial parallel manipulator is developed to show how a simple change in the structure targets a significant change in the singular regions inside the workspace [8, 9].

The following objectives are addressed in this article:

– to understand the behavior of the singularity region in a workspace;

– to understand the singularity behavior in parallel and serial manipulators.

2 Literature Review

Many research works in workspace singularities highlight the significance of the problem statement. Particularly, research works [10–12] explained the concept of prismatic actuators and the effect of singularities in the workspace. The presence of rotational actuators allowed singularities to develop inside the workspace. Adding each rotary joint in the manipulator leads to a proportional increase in the singular region inside the workspace. Öltjen et al. [13] concluded that redundancy reduces singularity possibilities.

Fontes and da Silva [14] developed a model of the parallel manipulator, where the base of each arm of the parallel manipulator was mounted on the linear prismatic joints, i.e., on the redundant links to provide a much more reliable singularity-free workspace of the manipulator.

In the further development of the work by Silva et al. [15], an experimental analysis of the redundant manipulator kinematics for the nature of energy consumption with the 3PRRR manipulator. The PR joint in the manipulator was redundant in the system.

Mostashiri et al. [16] showed that a redundant manipulator problem describes infinite solutions. The major problem with a spatial parallel manipulator is less or minimal singularity-free workspace. Parallel manipulators have many advantages compared to robot manipulators' disadvantages [17]. Due to this, many large load-carrying applications are using parallel manipulators.

Singularities in robotics refer to specific configurations or joint positions where the robot's end-effector (the part of the robot that interacts with the environment) loses one or more degrees of freedom, resulting in a breakdown or loss of control [18]. This effect can occur when the robot's links or joints become aligned to create a mathematical singularity, leading to instability, inaccuracy, and even complete loss of control [19]. These singularities can be particularly problematic in applications where precision, safety, and reliability are paramount, such as in medical robotics, aerospace, and industrial automation [20].

Briot and Goldsztejn [21] identified two types of singularities. Villalobos et al. [22] suggested the FSM method to handle singularities. Stejskal et al. [23] applied the Monte Carlo method to calculate singularity. Kieffer [24] studied the RCRCR mechanism singularities. Sakurai and Katsura [25] studied the static singularity solutions. Therefore, singularity is still a significant problem in current mechanisms and robotics.

The singularity avoidance is the gap considered in the 3PRPPS mechanism, and these manipulator arms are replaced with the circularly guided base. The end effector motions are observed in various ways with Matlab simulations and multi-body simulation software. The robot end effector of the 3PRPPS mechanism shows no singularity due to the circular guide base.

The singularity problem is proposed to be eliminated by solving the following objectives:

– to develop a new mechanism by modifying the existing mechanism; the fixed base should be replaced with a circular guide;

– new mechanism in a Jacobian matrix should be derived with direct kinematic relations;

– to calculate the workspace of the manipulator;

– to trace the pose of the end effector to identify singularities and singular free workspace.

3 Research Methodology

3.1 The proposed model- 3 PRPPS spatial parallel robot

The 3-PRPPS spatial parallel is modeled as shown in Figure 1.

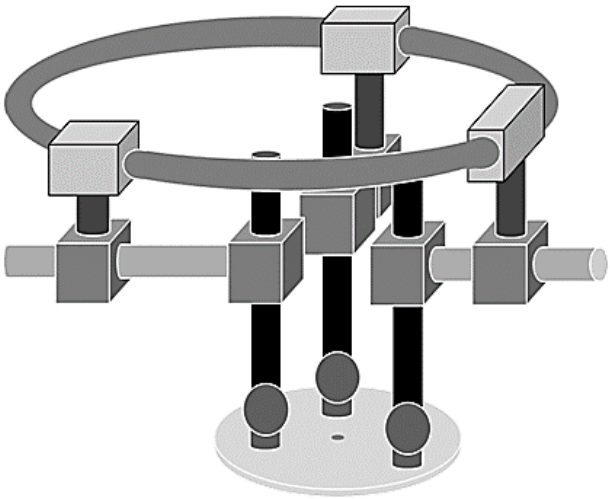

Figure 1 – The proposed 3-PRPPS Spatial parallel manipulator

Various methods for removing the singularity in the workspace were studied, including actuation and kinematic redundancy. Among these two methods of solving the problem of avoiding singularity, the kinematically redundant robots perform precisely, have lower energy consumption, and increase the manipulator's stiffness.

This article explains the robot manipulator, from its construction to how the manipulator works. It is essential to know the robot's construction to understand how it works during precision operations and avoid the singular configuration during the operation of the manipulator.

The robot follows both polar and Cartesian coordinate systems (Figure 2) to achieve the end effector position.

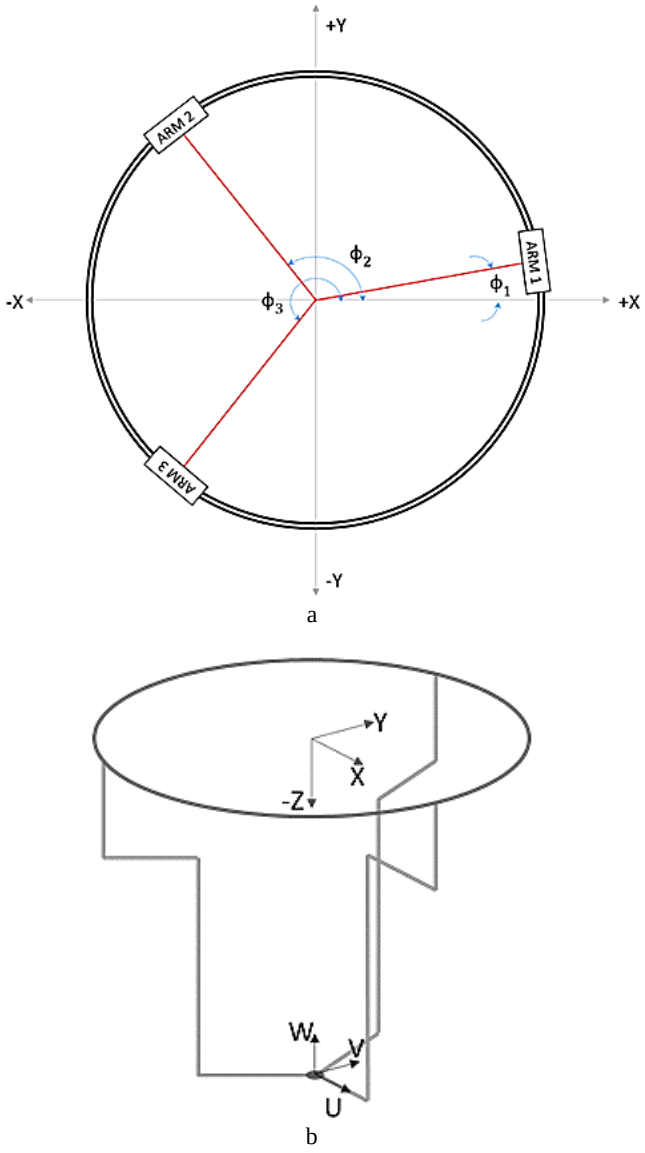

Figure 2 – Coordinate systems: a – orientations of the base of three arms along the circular base; b – global and end-effector Cartesian coordinates in 3D space

Initially, a polar coordinate system is used to position the reference frame, and the following frames follow the Cartesian coordinate to have a coordinated performance for a singular free workspace.

The polar coordinate system in the 3-PRPPS parallel manipulator allows the robot to actuate the base to position itself along the non-singular configurations. The parallel manipulator's possible configurations with a singular orientation are predetermined. Along the motion of the base frame, during singular conditions, the base is rotated along the circular guide to position it in such orientations where singularity does not exist.

The three arms of the manipulator are positioned along the circular base with radius RG and angles ϕ_1, ϕ_2, and ϕ_3 from the center, respectively (Figure 2a). This is a global reference frame of the entire robot manipulator, and it is a reference frame for retaining the original positions of the manipulators during actuation.

The 3D space of the Cartesian coordinate system is implemented in the workspace (Figure 2b). The robot's base frame / the reference frame in the polar system is considered the origin of the entire Cartesian system where the circular base is considered to move along the circular base through all four quadrants.

A robot with several links has various kinds of joints. Each joint has its nature of orientation in the 3D space. A joint's degree of freedom (DOF) is determined by the modes of restrictions that it has during actuation. Figure 3 represents the DOF motions the robot has relative to its joints.

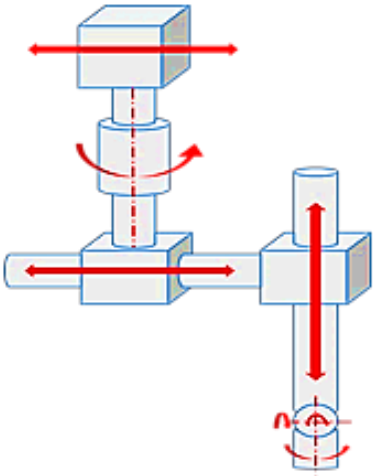

Figure 3 – DOF for the individual arm

The relative DOF of the robot is found by using the spatial DOF of a mechanism in its 3D space. The DOF of a spatial mechanism is calculated from the Chebychev–Grübler–Kutzbach criterion [26]:

$$DOF = 6(l-1) - \sum_{i=1}^{5}(6-i)P_i - F_R, \qquad (1)$$

where l – the number of of moving bodies; P_i – the number of i-th links; F_R – the number of joints.

A manipulator workspace is defined as the mobility region that can be found for each arm of the robot manipulator separately, forming a unique region bounded by a singular curve separating the region where the arm's mobility is restricted. For the points located inside this workspace, the manipulator has a similar inverse kinematic solution, and for the points located on this curve, the solution of the inverse kinematics of the robot manipulator is unique and requires special care since the two branches of the workspace meet at this curve.

The workspace of the proposed robot manipulator is obtained by setting the actuator lengths to their extreme positions, i.e., the maximum and the minimum value that

a link of the arm can take during its motion. The intersection of the mobility region of the arms obtains the workspace of the manipulator (Figure 4).

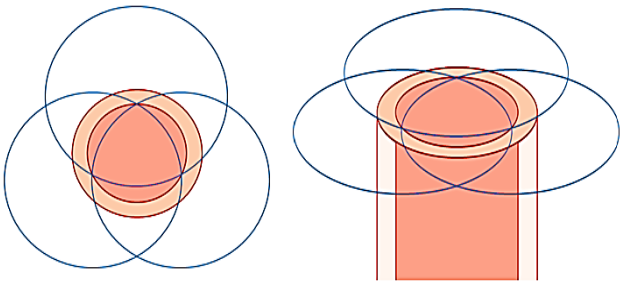

Figure 4 – Mobility regions of the arms of the manipulator along the X-Y plane and spatial configuration

The common region of the three circles is shown in spatial and planar space. Depicted regions are annular in the X-Y plane and can be expressed in the form of the equation as follows:

$$(x - x_i)^2 + (y - y_i)^2 = l_{3i\,max}^2; \quad x_i = l_{3i}\,cos(\theta_i)\,;\; y_i = l_{3i}\,sin(\theta_i)\,. \tag{2}$$

At each instantaneous position along the vertical axis, i.e., along the Z-axis, the robot follows the same workspace as in the planar configuration. Using the prismatic actuators along the vertical axis makes it possible to justify the work volume along the Z-axis.

During the actuation of the manipulator, the singular points occur in the workspace for the manipulator's arms configuration.

Initially, the orientation of the base of the arms of the manipulator during the robot's construction was discussed. This orientation of the arms plays a vital role in positioning the manipulator to avoid singular configurations during actuation. The orientation of the base along the circular guide is changed when the singularity is predetermined for the configuration in the workspace.

For reference, the polar system positions are used. The position of the base is changed regarding Arm 1 during actuation, and calculations for the orientation of the end effector are considered with the relation between the angle of the arms from Arm 1, considering Arm 1 is always on the X-axis. These positioning conditions of the proposed manipulator ensure that the end effector is never configured in its singular configuration.

3.2 Kinematics of the mechanism

The inverse kinematics is analyzed for a known end position of the end effector. The solution to the inverse kinematics provides the actuator positions of the links and joints. The manipulator is designed to divide its mechanisms into planar and spatial configurations. The orientation of the end effector is specified based on its required rotation in 3D space.

A rotation matrix is derived from the desired orientation of the end effector, which the operator defines during operation.

The flowchart shown in Figure 5 explains the procedure for determining the proposed manipulator's inverse kinematic solution.

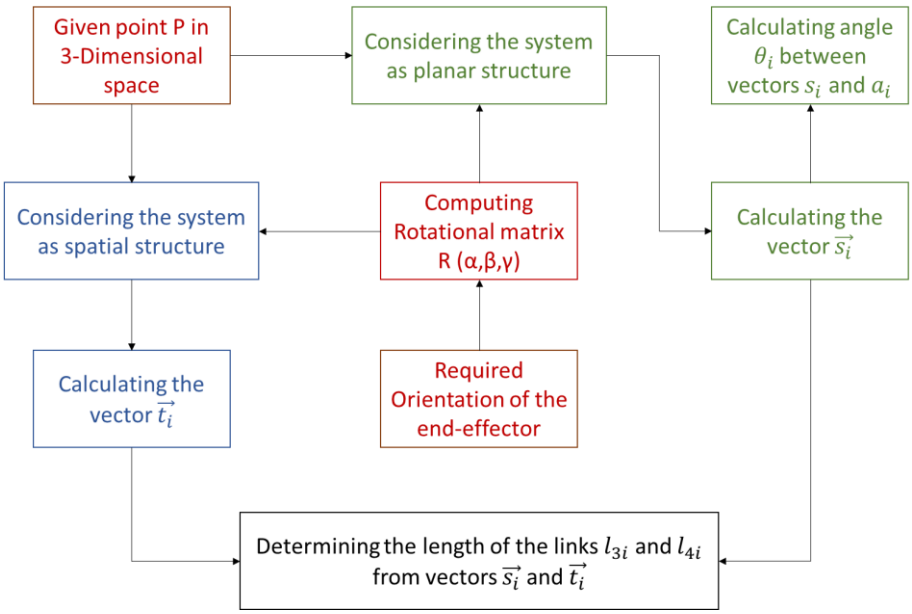

Figure 5 – Flow chart for Inverse kinematic function of the proposed parallel manipulator

The proposed robot's kinematics is studied using vector algebra for more straightforward calculations of the variables. The 3D robot's vector space is designed in two steps. The workspace is divided into 2 projections with respect to the global work frame, X-Y and Y-Z orientations.

Initially, the X-Y orientation is studied considering the planar orientations of the robot.

The planar configuration of the robot and leg configuration is shown in Figure 6. Spatial configuration is shown in Figure 7.

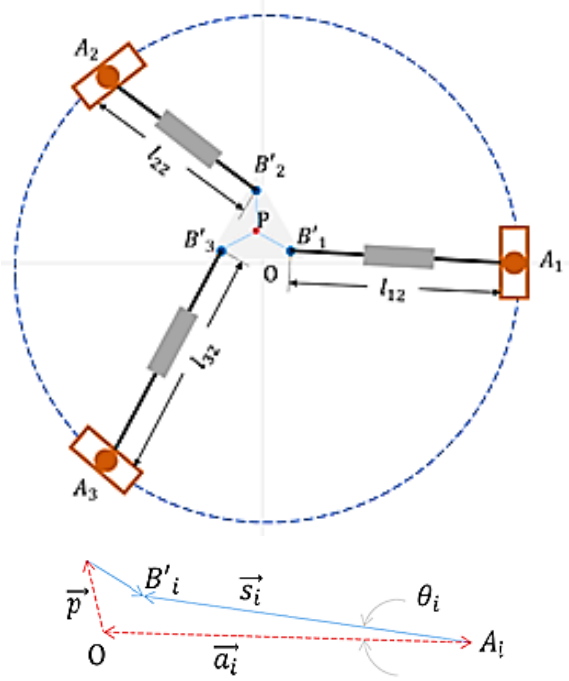

Figure 6 – Construction of the robot and arm considering its planar configuration

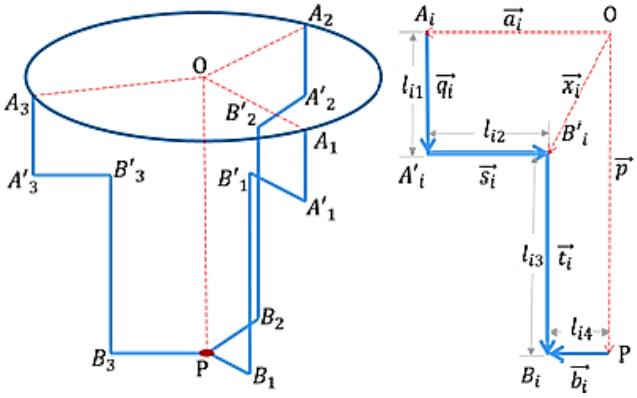

Figure 7 – Configuration of the robot in its spatial structure

The mathematical relations are developed from forward kinematic relations, and the Jacobian matrix is derived for position and orientation.

The single arm of the robot is converted into vector form to solve unknown variables in the following way. Solving this orientation of the robot gives the following equations:

$$\begin{gathered}\overrightarrow{OA_1}+\overrightarrow{A_1B_1}=\overrightarrow{OP}+\overrightarrow{PB_1};\\ \overrightarrow{a_1}+\overrightarrow{s_1}=\overrightarrow{p}+\overrightarrow{b_{01}};\\ \overrightarrow{b_{01}}=R_1^0\cdot\overrightarrow{b_1};\\ \overrightarrow{a_1}+\overrightarrow{s_1}=\overrightarrow{p}+R_1^0\cdot\overrightarrow{b_1},\end{gathered}$$

or in a general form:

$$\overrightarrow{a_1}+\overrightarrow{s_1}=\overrightarrow{p}+R\cdot\overrightarrow{b_1}, \tag{3}$$

where $\overrightarrow{a_1}$ – vector between the origin of the reference frame and the base frame at point A_i; $\overrightarrow{s_1}$ – vector between the points A and B, which changes the length AB, determining the position of the floating frame; $\overrightarrow{b_1}$ – vector between the working point and contact point of the floating frame at point B_i; $\vec{p}$ – vector between the working point and the origin of the reference frame.

Notably, $\overrightarrow{a_1}$ and $\overrightarrow{b_1}$ are predefined during the construction of the robot, and $\overrightarrow{p}$ is the required point with respect to the reference frame.

The only unknown variable $\overrightarrow{s_1}$ is determined from (3):

$$\overrightarrow{s_1}=\overrightarrow{p}+R\cdot\overrightarrow{b_1}-\overrightarrow{a_1}. \tag{4}$$

Solving equation (3) using the rotation matrix (4) results in a solution of the value of the unknown variable $\overrightarrow{s_i}$.

The angle θ_i is calculated using the following equation, according to the dot product relation for the angle between two vectors:

$$\theta_i=arccos\left(\frac{\overrightarrow{s_i}\cdot\overrightarrow{a_i}}{|\overrightarrow{s_i}|\cdot|\overrightarrow{a_i}|}\right). \tag{5}$$

The Y-Z plane is considered for solving the other variables using vector algebra for the spatial orientations.

The single arm of the robot is converted into vector form to solve unknown variables in the following way. Solving this orientation of the robot gives the following equations:

$$\begin{gathered}\overrightarrow{OB_i}+\overrightarrow{B'_iB_i}=\overrightarrow{OP}+\overrightarrow{PB_i};\\ \overrightarrow{x_i}+\overrightarrow{t_i}=\vec{p}+\overrightarrow{b_{0i}};\\ \overrightarrow{b_{0i}}=R_i^0\cdot\overrightarrow{b_i};\\ \overrightarrow{x_i}+\overrightarrow{t_i}=\vec{p}+R_i^0\cdot\overrightarrow{b_i},\end{gathered} \tag{6}$$

where $\overrightarrow{x_i}$ – vector between the origin of the reference frame and point B'_i; $\overrightarrow{t_i}$ – vector between points B'_i and B_i.

Notably, $\overrightarrow{a_i}$ and $\overrightarrow{q_i}$ are predefined vectors; $\overrightarrow{b_i}$ is obtained from equation (3); $\overrightarrow{x_i}$ is obtained by solving using the known variables:

$$\overrightarrow{x_i}=\vec{a}+\overrightarrow{q_i}+\overrightarrow{s_i}. \tag{7}$$

Also, the unknown variable $\overrightarrow{t_i}$ is obtained as follows:

$$\overrightarrow{t_i}=\vec{p}+R\overrightarrow{b_i}-\overrightarrow{x_i}. \tag{8}$$

Equation (8) contains the same rotational matrix (4).

3.3 The Jacobian matrix

The Jacobian matrix of the robot in its planar configuration is as follows. From the closed-loop kinematic chains $O-A_i-B'_i-P-O$ $(i=\{1,2,3\})$, the position column-vector p of the point P can be expressed in the base frame (Figure 8):

$$p=\begin{bmatrix}p_x\\p_y\end{bmatrix}=a_i+(b_i-a_i)+(p-b_i), \tag{9}$$

where a_i and b_i – position vectors of points A_i and B'_i, expressed in the base frame.

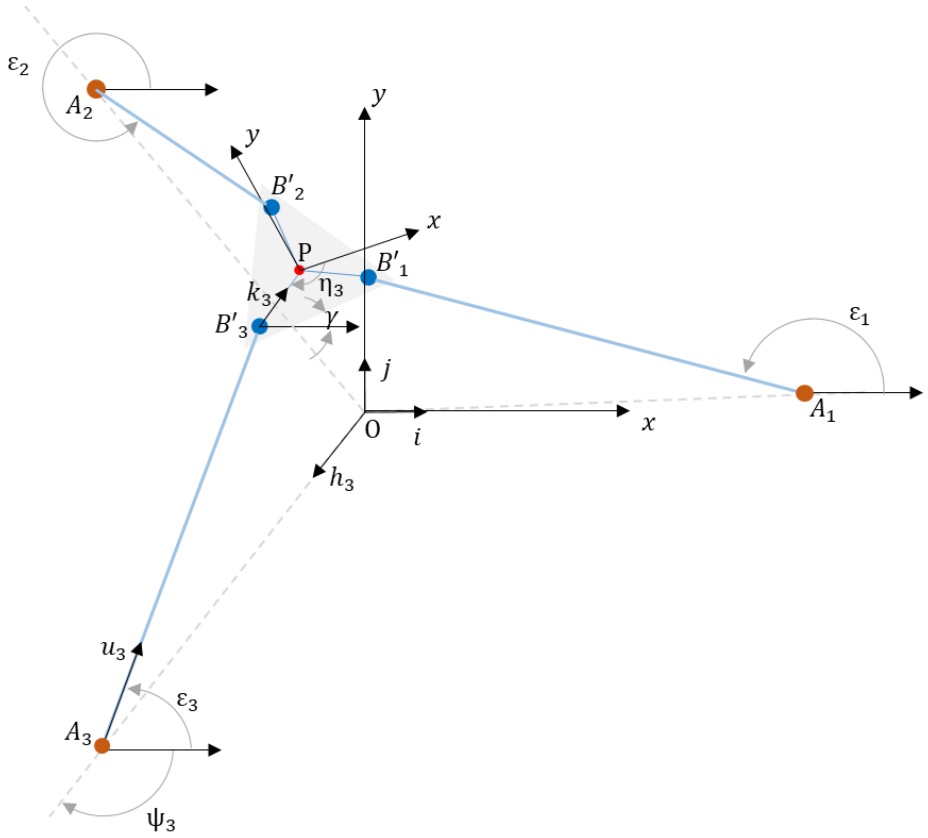

Figure 8 – 3-PRPPS manipulator in the planar configuration

Equation (9) can be written as follows:

$$\begin{gathered} p = a_i h_i + s_i u_i + b_i k_i; \\ h_i = \begin{bmatrix} cos\psi_i \\ sin\psi_i \end{bmatrix};\ u_i = \begin{bmatrix} cos\varepsilon_i \\ sin\varepsilon_i \end{bmatrix}; \\ k_i = \begin{bmatrix} cos\ (\gamma + \eta_i + \pi) \\ sin\ (\gamma + \eta_i + \pi) \end{bmatrix}, \end{gathered} \tag{10}$$

where a_i – the distance between points O and A_i; s_i – the distance between points A_i and B'_i; b_i – the distance between points B'_i and P.

Equation (10) also includes three unit vectors:

$$h_i = \frac{OA_i}{||OA_i||_2};\ u_i = \frac{A_iB'_i}{||A_iB'_i||_2};\ k_i = \frac{B'_iP}{||B'_iP||_2}.$$

Equation (10) can be rewritten in variations marked with "δ" sign:

$$\begin{gathered} \delta p = \delta a_i h_i + a_i \delta\psi_i E h_i + \delta s_i u_i + s_i \delta\varepsilon_i E u_i + \\ + \delta b_i k_i + b_i(\delta\gamma + \delta\eta_i) E k_i; \\ E = \begin{bmatrix} 0 & -1 \\ 1 & 0 \end{bmatrix}. \end{gathered} \tag{11}$$

After dot multiplying equation (11) by $s_i {u_i}^T$, it can be obtained:

$$\begin{gathered} s_i {u_i}^T \delta p = s_i \delta a_i {u_i}^T h_i + s_i a_i \delta\psi_i {u_i}^T E h_i + \\ + s_i \delta s_i + s_i \delta\varepsilon_i {u_i}^T E u_i + s_i \delta b_i {u_i}^T k_i + \\ + s_i b_i (\delta\gamma + \delta\eta_i) {u_i}^T E k_i, \end{gathered} \tag{12}$$

or in a vector form:

$$\begin{gathered} \boldsymbol{A}\begin{bmatrix} \delta a \\ \delta p \end{bmatrix} = H_a \begin{bmatrix} \delta a_1 \\ \delta a_2 \\ \delta a_3 \end{bmatrix} + H_\psi \begin{bmatrix} \delta\psi_1 \\ \delta\psi_2 \\ \delta\psi_3 \end{bmatrix} + \boldsymbol{B}\begin{bmatrix} \delta s_1 \\ \delta s_2 \\ \delta s_3 \end{bmatrix} + \\ + H_b \begin{bmatrix} \delta b_1 \\ \delta b_2 \\ \delta b_3 \end{bmatrix} + H_\eta \begin{bmatrix} \delta\eta_1 \\ \delta\eta_2 \\ \delta\eta_3 \end{bmatrix}; \\ \boldsymbol{A} = \begin{bmatrix} m_1 & s_1 {u_1}^T \\ m_2 & s_2 {u_2}^T \\ m_3 & s_3 {u_3}^T \end{bmatrix};\ \boldsymbol{B} = \begin{bmatrix} s_1 & 0 & 0 \\ 0 & s_2 & 0 \\ 0 & 0 & s_3 \end{bmatrix}; \\ m_i = -s_i b_i {u_i}^T E k_i\ (i = \{1,2,3\}); \\ H_a = diag[s_1 {u_1}^T h_1 s_2 {u_2}^T h_2 s_3 {u_3}^T h_3]; \\ H_\psi = diag[s_1 a_1 {u_1}^T E h_1 s_2 a_2 {u_2}^T E h_2 s_3 a_3 {u_3}^T E h_3]; \\ H_b = diag[s_1 {u_1}^T k_1 s_2 {u_2}^T k_2 s_3 {u_3}^T k_3]; \\ H_\eta = diag[s_1 b_1 {u_1}^T E k_1 s_2 b_2 {u_2}^T E k_2 s_3 a_3 {u_3}^T E k_3], \end{gathered} \tag{13}$$

where $\boldsymbol{A}$ and $\boldsymbol{B}$ – direct and inverse Jacobian matrices of the manipulator, respectively, in its planar configuration.

Assuming that $\boldsymbol{A}$ is non-singular, i.e., the manipulator does not meet singular configurations of the 2nd type.

Multiplying equation (13) with $\boldsymbol{A}^{-1}$ and introducing the Jacobian matrices

$$\begin{gathered} J_a = \boldsymbol{A}^{-1} H_a; J_\psi = \boldsymbol{A}^{-1} H_\psi;\ J = \boldsymbol{A}^{-1}\boldsymbol{B}; \\ J_b = \boldsymbol{A}^{-1} H_b; J_\eta = \boldsymbol{A}^{-1} H_\eta \end{gathered} \tag{14}$$

allows for obtaining the following:

$$\begin{bmatrix}\delta a\\ \delta p\end{bmatrix} = J_a \begin{bmatrix}\delta a_1\\ \delta a_2\\ \delta a_3\end{bmatrix} + J_\psi \begin{bmatrix}\delta \psi_1\\ \delta \psi_2\\ \delta \psi_3\end{bmatrix} + \\ + J \begin{bmatrix}\delta s_1\\ \delta s_2\\ \delta s_3\end{bmatrix} + J_b \begin{bmatrix}\delta b_1\\ \delta b_2\\ \delta b_3\end{bmatrix} + J_\eta \begin{bmatrix}\delta \eta_1\\ \delta \eta_2\\ \delta \eta_3\end{bmatrix}. \quad (15)$$

Notably, J is the kinematic Jacobian matrix of the manipulator; the matrices J_a, J_ψ, J_b, and J_η are the sensitivity coefficients of the position and orientation of the end effector variations in the polar coordinates of the points A_i and B'_i.

In the proposed manipulator, link 4 is prismatic and has lower or no singular points along the vertical axis.

The orientation of the end effector along the rotations in the X and Y axes, i.e., the changes in the angles α and β, respectively, are restricted to a magnitude of axial rotations based on the selected spherical joint. At the maximum, the permissible rotation on the spherical joint varies from 0–60° magnitude.

4 Results

The use of Cartesian links in the spatial configurations of the robot does not need any calculations of kinematically singular points along the vertical motion. The restrictions of the actuators are only found when there is a presence of rotational joints, i.e., used to orient the manipulator along the X and Y axes with rotations along the Z-axis. Singular points are affected majorly along the X and Y axes only. These equations are solved in Matlab, and the path of the end effector is generated for various positions and orientations.

The results were obtained during the validation process of the proposed parallel manipulator. The singular free movement of end effectors is recorded in the 3D workspace to avoid all types of singularities (Figures 9, 10).

3-PRPPS spatial parallel manipulator is also modeled in MSC Adams software to understand the dynamics of the manipulator. Initially, the links are defined in the software for the proposed manipulator (Figures 11, 12).

Joint actions are defined as required in the corresponding joints. The timed functions are defined in the joints one by one to understand the dynamic nature of the manipulator in real-time.

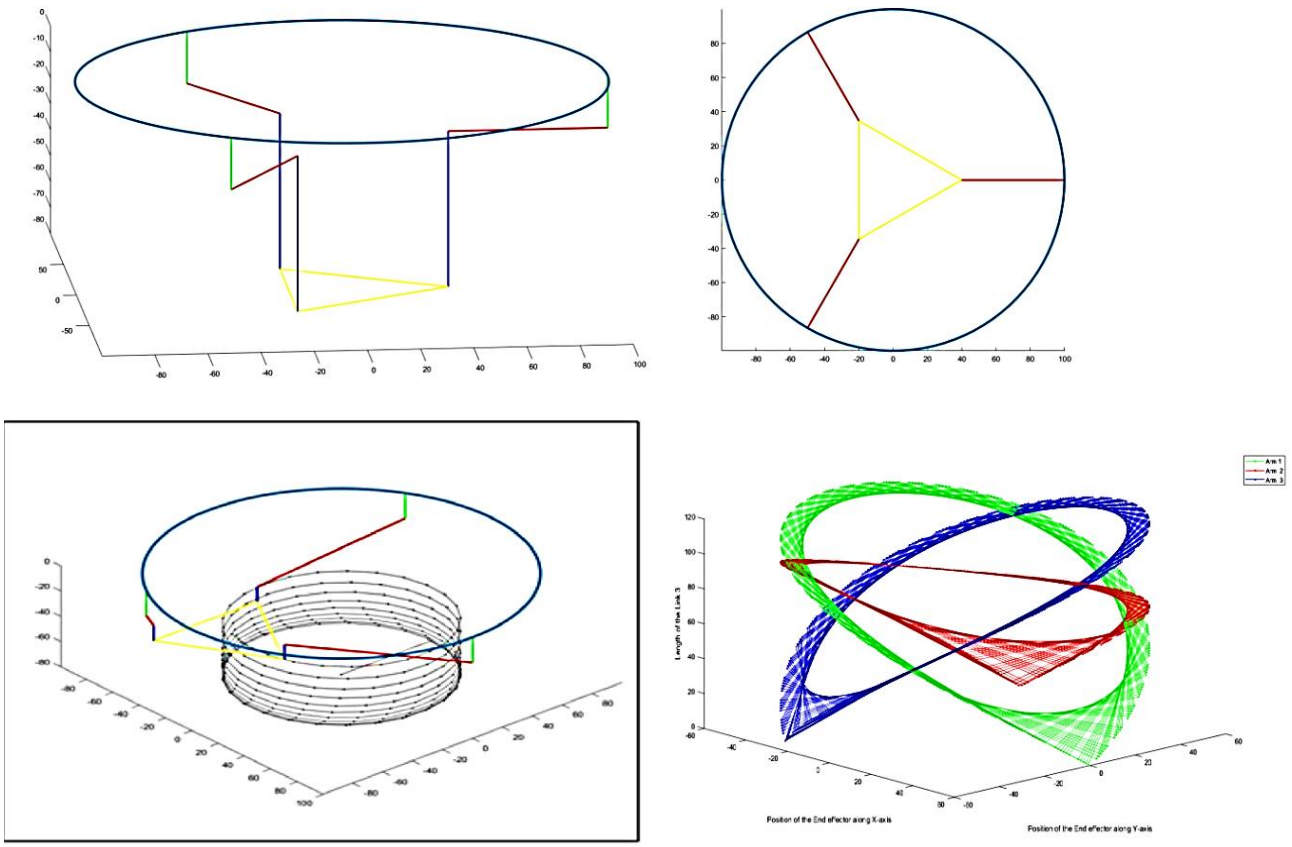

Figure 9 – Different orientations of the robot manipulator

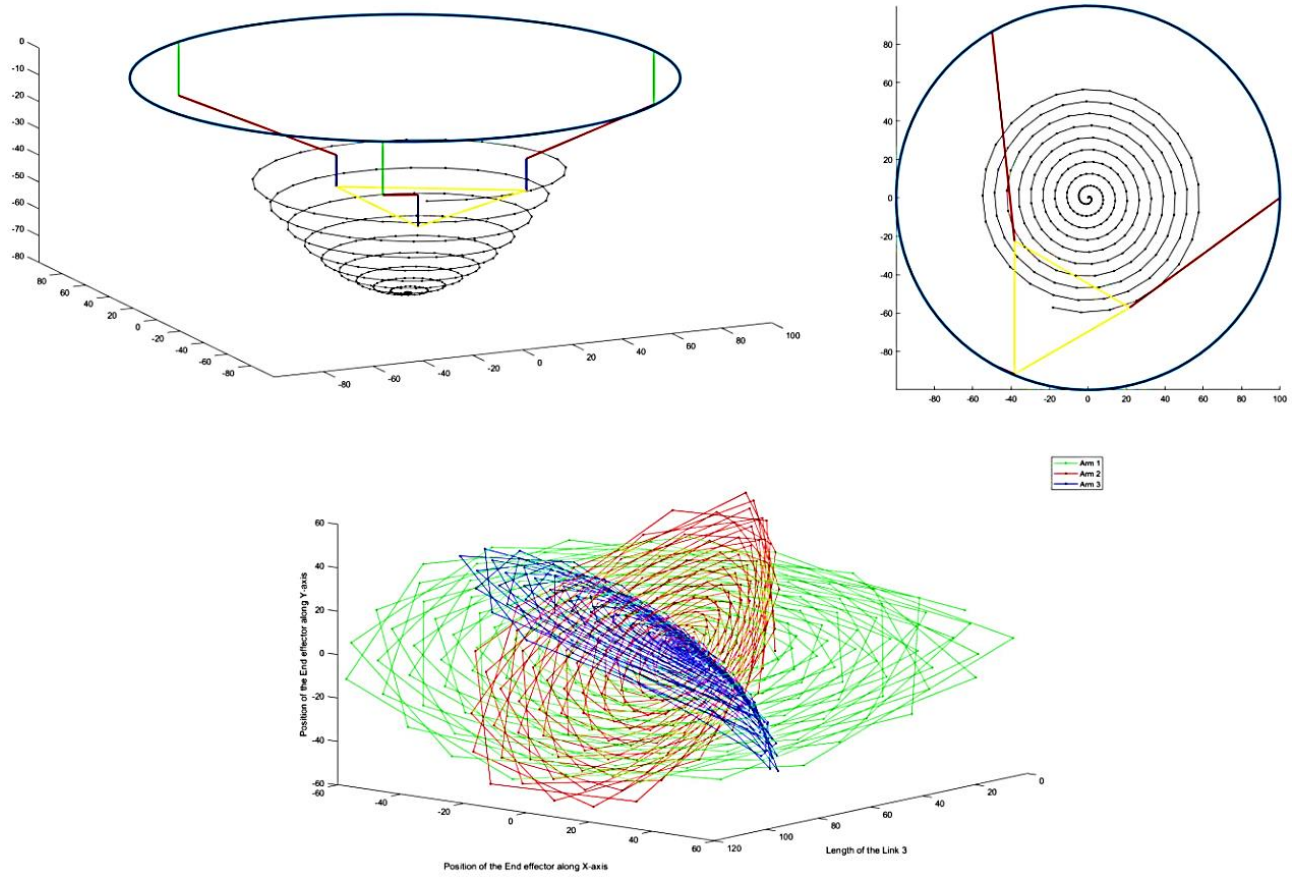

Figure 10 – Changes in the length of link 3 of the robot manipulator for the spiral path represented

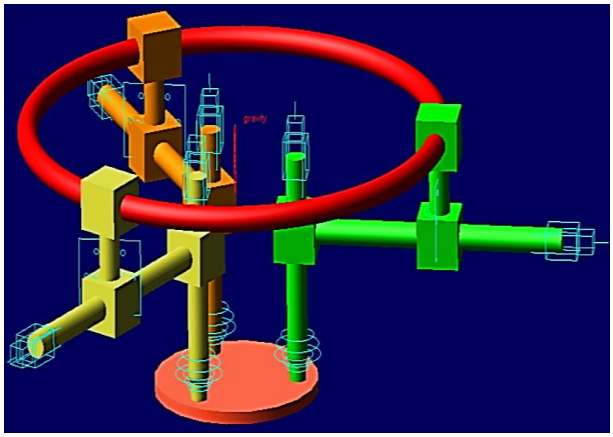

Figure 11 – Link configurations used for validation in MSC ADAMS

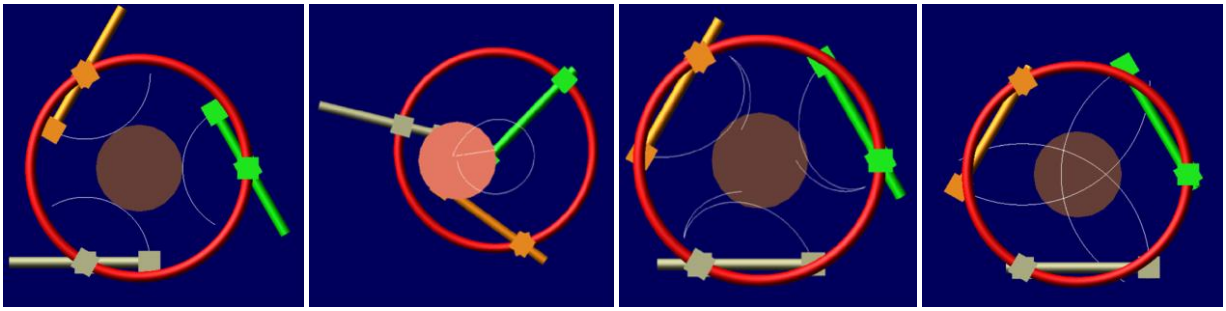

Figure 12 – Different positions and orientations of the manipulator

5 Discussion

The values were obtained in both Matlab and MSC Adams software. Matlab software is made to validate the results in the mathematical equations with respect to the inverse kinematic solutions.

On the other hand, in the MSC Adams software, the joint motions are applied to understand the end effector positions, i.e., the manipulator's forward kinematics is studied.

The 3-PRPPS parallel spatial manipulator was constructed mathematically in Matlab to perform the inverse kinematic solutions. Different orientations of the robot manipulator are shown in Figure 9.

Various paths were constructed so the manipulator could follow and understand the changes in the length of the links. For the path, the values of X and Y increment by value 1 over a period of –60 to 60. The changes in the link lengths are studied and plotted in the graph, along with the positions in the X and Y axes separately.

The following was obtained from the dynamic analysis using the MSC Adams software. The motion of the end effector along the X-Y plane where the arms are initially extended to a required horizontal position and then guide prismatic link is actuated to form a circular path.

This proves the ability of the manipulator to manipulate the workspace into its required orientations to reach a required position. Through this manipulator working mechanism, any complex trajectory can be planned accordingly.

6 Conclusions

The article proposes a new mechanism, i.e., 3PRPPS, which contains three prismatic joints, one revolute, and one spherical joint. The robot mechanism has been modeled with direct kinematic relations. The 3PRPPS spatial manipulator's fixed base is replaced with a circular guide. The end effector motion has been studied.

During the motion, singularities have not been found. The total workspace is singular-free. The behavior of the singularity region in the confined workspace has been studied carefully to operate with the behavioral nature of the links and joints in the parallel manipulators and finalize the configuration of the robot manipulator.

Singularities are categorized into three types; all three singularity types have been considered for carefully avoiding the singular configurations during the actuation of the links in the workspace. The position and orientation configurations have been explained to understand the singularity-free pose of the end effector and achieve maximum utilization of the workspace.

Using prismatic joints in a parallel manipulator helps reduce singular zones in the workspace. The manipulator's customisability in every aspect helps to fit it into industrial applications.

There are requirements for precise and continuous path planning in the industry. The proposed parallel manipulator can achieve the applications. Currently, functioning parallel manipulators can be replaced with the same design concept to achieve maximum utilization of the available singular-free workspace and the complex trajectories inside the workspace.

References

1. Pfeiffer, K. (2019). *Efficient Kinematic and Algorithmic Singularity Resolution for Multi-Contact and Multi-Level Constrained Dynamic Robot Control*. DSc. thesis, Université Montpellier, Montpellier, France.
2. Visinsky, M.L., Cavallaro, J.R., Walker, I.D. (1994). Robotic fault detection and fault tolerance: A survey. *Reliability Engineering & System Safety*, Vol. 46(2), pp. 139–158, https://doi.org/10.1016/0951-8320(94)90132-5
3. Titus, N.A. (1998). Singularity avoidance strategies for satellite mounted manipulators using attitude control. Ph.D. thesis. Air Force Institute of Technology, Wright-Patterson, OH, USA.
4. Bohigas, O., Manubens, M., Ros, L. (2016). *Singularities of Robot Mechanisms: Numerical Computation and Avoidance Path Planning*. Springer, Cham, Switzerland. https://doi.org/10.1007/978-3-319-32922-2
5. Pistone, A., Ludovico, D., Dal Verme, L.D.M.C., Leggieri, S., Canali, C., Caldwell, D.G. (2024). Modelling and control of manipulators for inspection and maintenance in challenging environments: A literature review. *Annual Reviews in Control*, Vol. 57, 100949. https://doi.org/10.1016/j.arcontrol.2024.100949
6. Yu, Q., Gravish, N. (2024). Multimodal locomotion in a soft robot through hierarchical actuation. *Soft Robotics*, Vol. 11(1), pp. 21–31. https://doi.org/10.1089/soro.2022.0198
7. Rodriguez-Guerra, D., Sorrosal, G., Cabanes, I., Mancisidor, A., Calleja, C. (2024). Singularity parametrization with a novel kinematic decoupled model for non-spherical wrist robots. *Journal of Mechanisms and Robotics*, Vol. 16(5), 051003. https://doi.org/10.1115/1.4062586
8. Li, W., Angeles, J. (2017). A novel three-loop parallel robot with full mobility: kinematics, singularity, workspace, and dexterity analysis. *Journal of Mechanisms and Robotics*, Vol. 9(5), 051003. https://doi.org/10.1115/1.4037112
9. Kaloorazi, M.H.F., Masouleh, M.T., Caro, S. (2016). Determining the maximal singularity-free circle or sphere of parallel mechanisms using interval analysis. *Robotica*, Vol. 34(1), pp. 135–149. https://doi.org/10.1017/S0263574714001271
10. Ryu, W., Kim, J., Kim, S., Choi, Y.J., Lee, S. (2021). Development of a parallel robotic positioning system with specific workspace for noninvasive brain stimulation. *IEEE/ASME Transactions on Mechatronics*, Vol. 27(5), pp. 2450–2461. https://doi.org/10.1109/TMECH.2021.3114852

11. Merlet, J.P. (2017). Simulation of discrete-time controlled cable-driven parallel robots on a trajectory. *IEEE Transactions on Robotics*, Vol. 33(3), pp. 675–688. https://doi.org/10.1109/TRO.2017.2664888
12. Merlet, J.P. (2016). A generic numerical continuation scheme for solving the direct kinematics of cable-driven parallel robot with deformable cables. *In: 2016 IEEE/RSJ International Conference on Intelligent Robots and Systems*, pp. 4337–4343. http://doi.org/10.1109/IROS.2016.7759638
13. Öltjen, J., Kotlarski, J., Ortmaier, T. (2016). On the reduction of vibration of parallel robots using flatness-based control and adaptive inputshaping. *In: 2016 IEEE International Conference on Advanced Intelligent Mechatronics*, pp. 695–702. https://doi.org/10.1109/AIM.2016.7576849
14. Fontes, J.V., da Silva, M.M. (2016). On the dynamic performance of parallel kinematic manipulators with actuation and kinematic redundancies. *Mechanism and Machine Theory*, Vol. 103, pp. 148–166. https://doi.org/10.1016/j.mechmachtheory.2016.05.004
15. Fontes, J.V.C., Vieira, H.L., da Silva, M.M. (2018). The impact of kinematic redundancies on the conditioning of a planar parallel manipulator. In: *Computational Kinematics: Proceedings of the 7th International Workshop on Computational Kinematics*, pp. 449–456. https://doi.org/10.1007/978-3-319-60867-9_51
16. Mostashiri, N., Dhupia, J.S., Verl, A.W., Xu, W. (2018). A review of research aspects of redundantly actuated parallel robotsw for enabling further applications. *IEEE/ASME Transactions on Mechatronics*, Vol. 23(3), pp. 1259–1269. https://doi.org/10.1109/TMECH.2018.2792450
17. Liang, D., Mao, Y., Song, Y., Sun, T. (2024). Kinematics, dynamics and multi-objective optimization based on singularity-free task workspace for a novel SCARA parallel manipulator. *Journal of Mechanical Science and Technology*, Vol. 38(1), pp. 423–438. https://doi.org/10.1007/s12206-023-1235-6
18. Marić, F., Petrović, L., Guberina, M., Kelly, J., Petrović, I. (2021). A Riemannian metric for geometry-aware singularity avoidance by articulated robots. *Robotics and Autonomous Systems*, Vol. 145, 103865. https://doi.org/10.1016/j.robot.2021.103865
19. Wang, H., Zhou, Z., Zhong, X., Chen, Q. (2022). Singular configuration analysis and singularity avoidance with application in an intelligent robotic manipulator. *Sensors*, Vol. 22(3), 1239. https://doi.org/10.3390/s22031239
20. Zhang, X., Fan, B., Wang, C., Cheng, X. (2021). Analysis of singular configuration of robotic manipulators. *Electronics*, Vol. 10(18), 2189. https://doi.org/10.3390/electronics10182189
21. Briot, S., Goldsztejn, A. (2021). Singularity conditions for continuum parallel robots. *IEEE Transactions on Robotics*, Vol. 38(1), pp. 507–525. https://doi.org/10.1109/TRO.2021.3076830
22. Villalobos, J., Sanchez, I.Y., Martell, F. (2022). Singularity analysis and complete methods to compute the inverse kinematics for a 6-DOF UR/TM-type robot. *Robotics*, Vol. 11(6), 137. https://doi.org/10.3390/robotics11060137
23. Stejskal, T., Svetlík, J., Ondočko, Š. (2022). Mapping robot singularities through the Monte Carlo method. *Applied Sciences*, Vol. 12(16), 8330. https://doi.org/10.3390/app12168330
24. Kieffer, J. (1994). Differential analysis of bifurcations and isolated singularities for robots and mechanisms. *IEEE Transactions on Robotics and Automation*, Vol. 10(1), pp. 1–10. https://doi.org/10.1109/70.285580
25. Sakurai, S., Katsura, S. (2024). Singularity-free 3-leg 6-DOF spatial parallel robot with actuation redundancy. *IEEJ Journal of Industry Applications*, Vol. 13(2), pp. 127–134. https://doi.org/10.1541/ieejjia.23003740
26. Morecki, A., Knapczyk, J. (2014). *Basics of Robotics: Theory and Components of Manipulators and Robots*. Springer, Cham, Switzerland. https://doi.org/10.1007/978-3-7091-2532-8